PERGAMON

Journal of Structural Geology 25 (2003) 1263–1279

JOURNAL OF STRUCTURAL GEOLOGY

www.elsevier.com/locate/jsg

The Jeremoabo transpressional transfer fault, Recôncavo–Tucano Rift, NE Brazil

Nivaldo Destro[a,*], Fernando F. Alkmim[b], Luciano P. Magnavita[c], Peter Szatmari[a]

[a]*Petrobras, Centro de Pesquisas, Cidade Universitária, Quadra 7, Ilha do Fundão, Rio de Janeiro (RJ), 21949-900, Brazil*
[b]*Departamento de Geologia, Escola de Minas, Universidade Federal de Ouro Preto, Morro do Cruzeiro, Ouro Preto (MG), 35400-000, Brazil*
[c]*Petrobras, Departamento de Exploração e Produção, Avenida Antônio Carlos Magalhães, 1113, Salvador (BA), 41856-900, Brazil*

Received 16 December 2001; received in revised form 1 October 2002; accepted 9 October 2002

Abstract

The Jeremoabo fault, located in the Early Cretaceous Recôncavo–Tucano Rift, northeastern Brazil, represents an example of transfer fault. A field-based structural analysis along 20 km of exposures revealed an E–W-trending and steeply dipping reverse-sinistral fault that resulted from transpressional reactivation of a pre-existent weak zone. The fault is associated with a 5-km-wide footwall deformation zone, in which sandstone layers are folded and locally overturned becoming parallel to the fault. The deformation zone contains a pervasive system of NE- and NNW-trending conjugate Riedel shear fractures of outcrop to kilometer scale. A paleostress analysis based on these Riedel fractures indicated σ_1 and σ_3 trending, respectively, 016° and 108°, and σ_2 subvertical, consistent with transpression and local switch between σ_1 and σ_2 relative to the regional paleostress field. The Jeremoabo fault links smaller rift border faults and has sense of slip consistent with the mapped offset of the basin border. Its transfer function is attested by linkage with a major dextral transfer fault and a transfer zone during the rifting period. By acting together these structures accommodated the change in asymmetry between the two major half-grabens of the rift.

Keywords: Tucano Rift; Jeremoabo fault; Transfer fault; Transpression; Riedel fractures; Oblique rift

1. Introduction

Transfer faults (Gibbs, 1984), originally described in rift basins, are cross-faults that accommodate differences in strain or structural styles along the strike of the extensional system (e.g. Lister et al., 1986; Milani and Davison, 1988; Bosworth, 1995; Salah and Alsharhan, 1996; McClay and Khalil, 1998). Faults with the same function have been also recognized in other tectonic settings, especially in fold-thrust belts. Rift transfer faults are portrayed in the literature as pure strike-slip faults, when parallel to the extension direction, or as oblique-slip faults, with variable amount of dip displacement, when oblique to the extension direction (Gibbs, 1984; Lister et al., 1986). Both compressive (transpressional) and extensional (transtensional) structures may develop along transfer faults, depending on their angular relationship with the components of the extensional system (Gibbs, 1984). Transfer faults usually connect major normal faults with similar or opposite polarities and their sense of slip is contrary to the apparent offset of the related normal faults (Gibbs, 1990).

Transpressional transfer faults have been rarely described in the literature. In this paper we present the Jeremoabo fault from the Cretaceous Recôncavo–Tucano Rift, northeastern Brazil (Fig. 1), as an example of a transpressional transfer fault. The basis for our study is a detailed structural analysis performed in 20 km of exposures along the Jeremoabo fault zone. Our data set indicates that the sinistral Jeremoabo fault nucleated and evolved during the rifting period in a local transpressional regime, acting as a transfer fault. Besides the transpressional character, we also noticed that the Jeremoabo fault does not connect major normal border faults, and the observed sense of slip is the same as the apparent offset of the related normal faults.

In the following sections, we describe the Jeremoabo fault and associated structures, provide an explanation for their development, and discuss the role they played in the evolution of the Tucano Rift. In addition, we demonstrate that the transpressional character of this peculiar transfer

* Corresponding author.
E-mail address: nivaldo@cenpes.petrobras.com.br (N. Destro).

0191-8141/03/$ - see front matter
PII: S0191-8141(02)00164-5

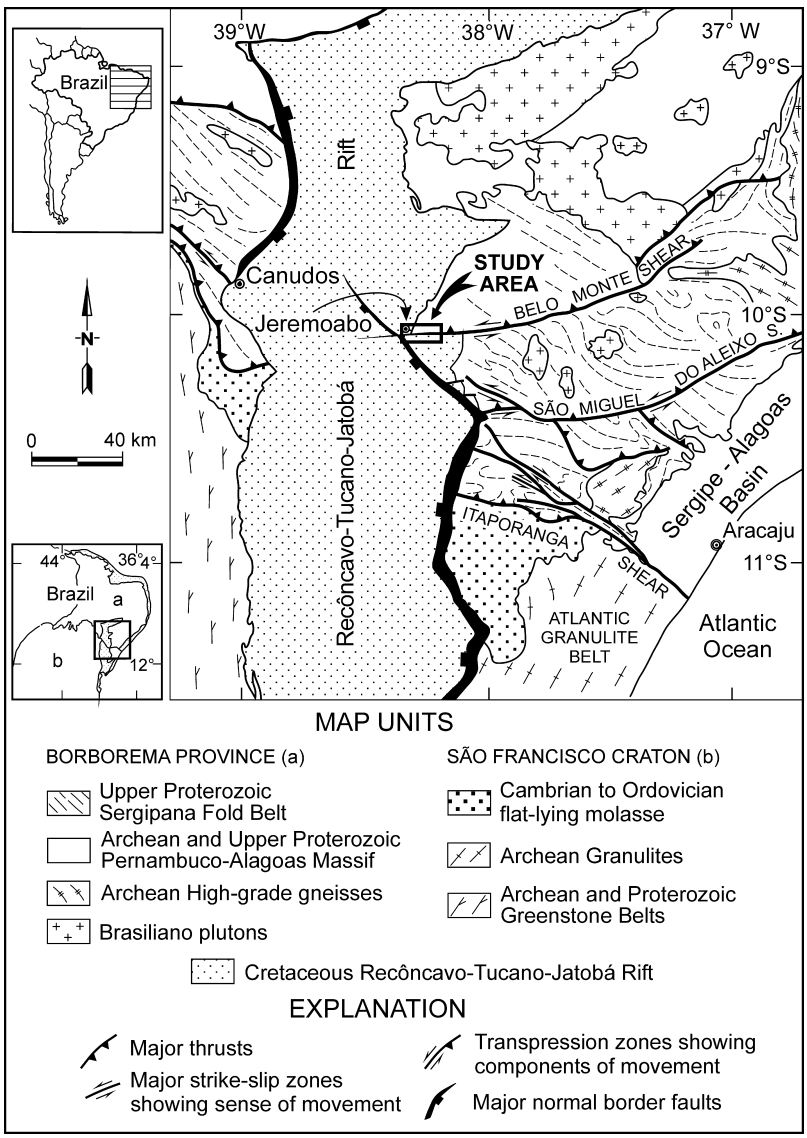

Fig. 1. Location of the study area (rectangle contour) in northeastern Brazil, within the Borborema Province. Major structures of the Precambrian basement adjacent to the Recôncavo–Tucano–Jatobá Rift (modified from Davison and Santos, 1989). The Jeremoabo fault lies along the western portion of the Precambrian Belo Monte shear zone. Inset maps show location of the Borborema Province and the São Francisco Craton in northeastern Brazil.

fault is a consequence of its nucleation on a pre-existing weak zone and the oblique nature of the Tucano Rift.

One of our major objectives in this study has been to differentiate transfer faults from another type of cross fault, release faults, which are genetically distinct, that is, geometrically, kinematically and dynamically. Whereas transfer faults connect normal faults, and horizontal motion predominates along them over dip-slip (Gibbs, 1984), release faults accompany a single major normal fault, and dip-slip predominates over horizontal motion (Destro, 1995; Destro et al., 2003). Distinctly from transfer faults, release faults form because varying vertical displacement along the strike of the controlling (parent) normal faults causes the hanging wall block to increase in length, and as the normal faults terminate laterally, some kind of cross fault is geometrically and mechanically necessary to accommodate this increase of length of the hanging wall (Destro, 1995; Destro et al., 2003). Destro et al. (2003) presented a study on release faults carried out in the Recôncavo Rift, the southernmost portion of the Recôncavo–Tucano–Jatobá Rift (Fig. 1). In this paper, new aspects of release faults are shown such as the development of structures associated with release faults, including release joints, shale diapirs and release faults of reverse character. An analysis of most of the hydrocarbon accumulations of the Recôncavo Rift in the context of the release faulting concept is also provided.

2. Geologic setting

The Jeremoabo fault is located on the eastern border of the Tucano Rift in northeastern Brazil (Fig. 1). The Tucano

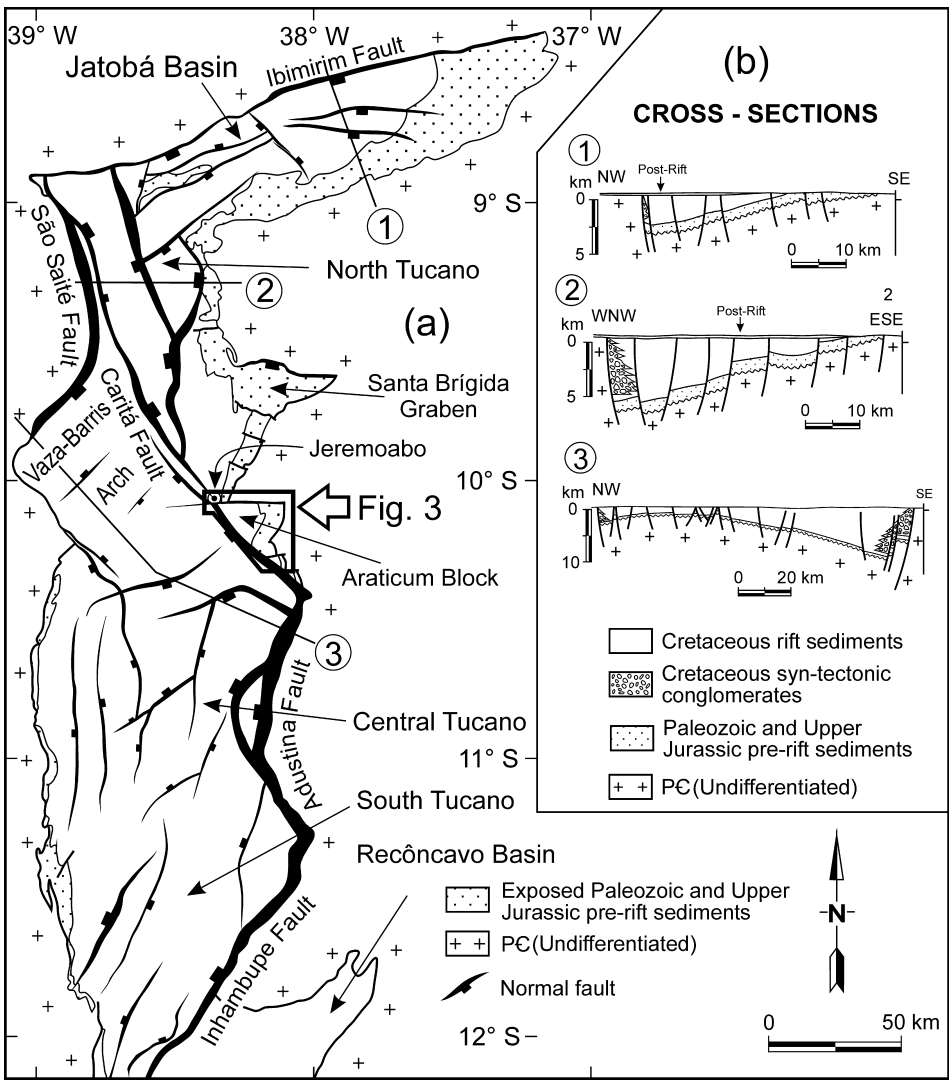

Fig. 2. (a) Simplified tectonic map to the top of the prerift Sergi Formation in the Tucano–Jatobá Rift (modified from Aragão and Peraro, 1994). The main regional features closely associated to the Jeremoabo fault, such as the Vaza-Barris Arch and the Araticum Block are shown. The basin border limits the Araticum Block to the east. The Jeremoabo fault and the Caritá faults limit this block, respectively, to the north and west. The study area lies along the Jeremoabo fault to the east from Jeremoabo Town. (b) Cross-sections illustrating the switch in the asymmetry of half-grabens between the Central and North Tucano Sub-basins (adapted from Magnavita, 1992).

Rift corresponds to the central portion of the Recôncavo–Tucano–Jatobá Rift, a Late Jurassic to Early Cretaceous system of continental half-grabens (Fig. 2) connected to the eastern Brazilian margin. Developed across the boundary between two major provinces of the Brazilian Shield, the São Francisco Craton and the Borborema Province (Almeida et al., 1981) (Fig. 1), the Recôncavo–Tucano–Jatobá Rift evolved as a failed rift arm during the break-up of Gondwana and opening of the South Atlantic (e.g. Szatmari et al., 1985, 1987; Milani et al., 1988; Szatmari and Milani, 1999). The São Francisco Craton is made up from Archean to Paleoproterozoic crustal rocks and is one of the portions of the South American continent not affected by the Neoproterozoic Brasiliano/Pan-African tectonism that led to the assembly of Gondwana. The Borborema Province, on the contrary, is a fold-thrust belt with a major strike-slip system generated in the course of the Neoproterozoic Brasiliano/Pan-African collision.

The most striking feature of the Tucano Rift is the reversal in the asymmetry of the half-grabens along its strike. In its southern portion, the rift border is located to the east; in its northern portion the master fault nucleated to the west (Fig. 2). A broad feature named Vaza-Barris Arch separates these two half-grabens. The Vaza-Barris arch interacted in a complex way with the Jeremoabo fault, and the dextral normal Caritá fault (Magnavita, 1992). The E–W-trending Jeremoabo fault is over 20 km long and connects offset segments of the eastern border of the Tucano Rift (Fig. 2). The portion of the Tucano Rift to the south of the Jeremoabo fault, an area referred to as Araticum Block (Fig. 3), is a relatively shallow basement block, overlain by Upper

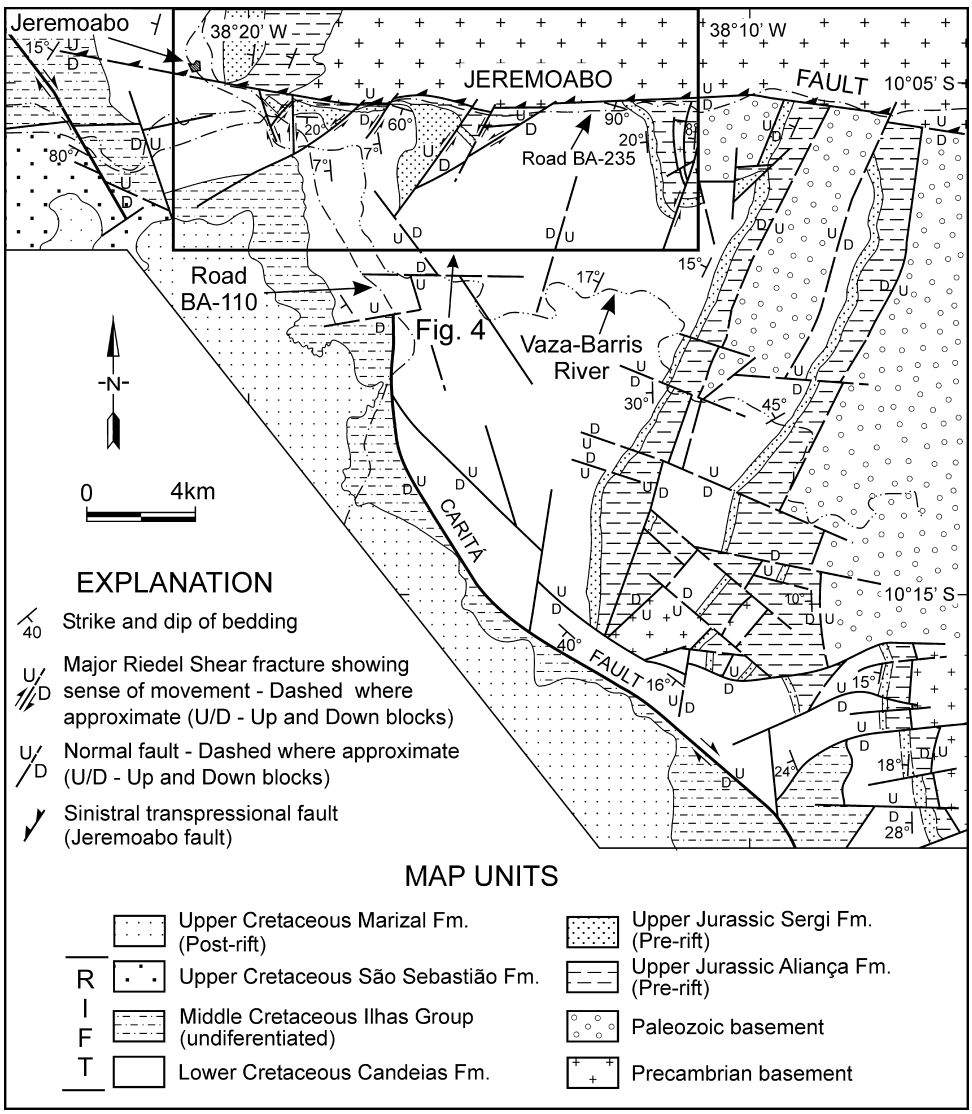

Fig. 3. Geologic map of the Araticum Block (modified from Magnavita and Cupertino, 1987).

Jurassic prerift sediments and a Lower Cretaceous rift sequence (Fig. 3).

Davison (1985) noted that the basement structures along the Jeremoabo fault probably mark the position of a Proterozic shear zone, named Belo Monte shear zone (Davison and Santos, 1989), one of the largest ductile shear zones of the Neoproterozic Sergipana Fold Belt (Davison and Santos, 1989) (Fig. 1). He recognized its curved E–W trend and inferred that the N–S faults that occur along it must have both normal and transcurrent slip components because the amount of throw varies greatly from one fault block to the next. He portrayed the Jeremoabo fault as a normal fault (Fig. 9). Magnavita (1992) inferred a component of sinistral movement for the Jeremoabo fault, based on the presence of the NE-trending sinistral Riedel fractures and the offset of the rift border. The data presented in this paper support some remarks of the above-mentioned authors and give a new insight into the tectonic evolution of this fault, as well as its role in the evolution of the Tucano Rift.

An overall NW–SE extensional direction has been determined for the Recôncavo–Tucano–Jatobá Rift (e.g. Szatmari et al., 1985; Szatmari et al., 1987; Milani and Davison, 1988; Milani et al., 1988; Szatmari and Milani, 1999). Magnavita (1992) deduced an E–W-oriented extension direction during Early Neocomian time, and a NW–SE-oriented extension direction during the Late Barremian/Early Aptian time. These works support the overall extensional setting of the rift, where σ_1 was vertical. The NW–SE extension direction has also been inferred in other Cretaceous rift basins of northeastern Brazil, such as the Sergipe–Alagoas Basin (Destro, 1995), and the Camamu Basin (Mercio, 1996). Since the Recôncavo–Tucano–Jatobá Rift has an overall N–S orientation, an oblique rift developed.

The age of the Jeremoabo fault is locally constrained as post-Late Jurassic to Early Aptian. Synrift sediments

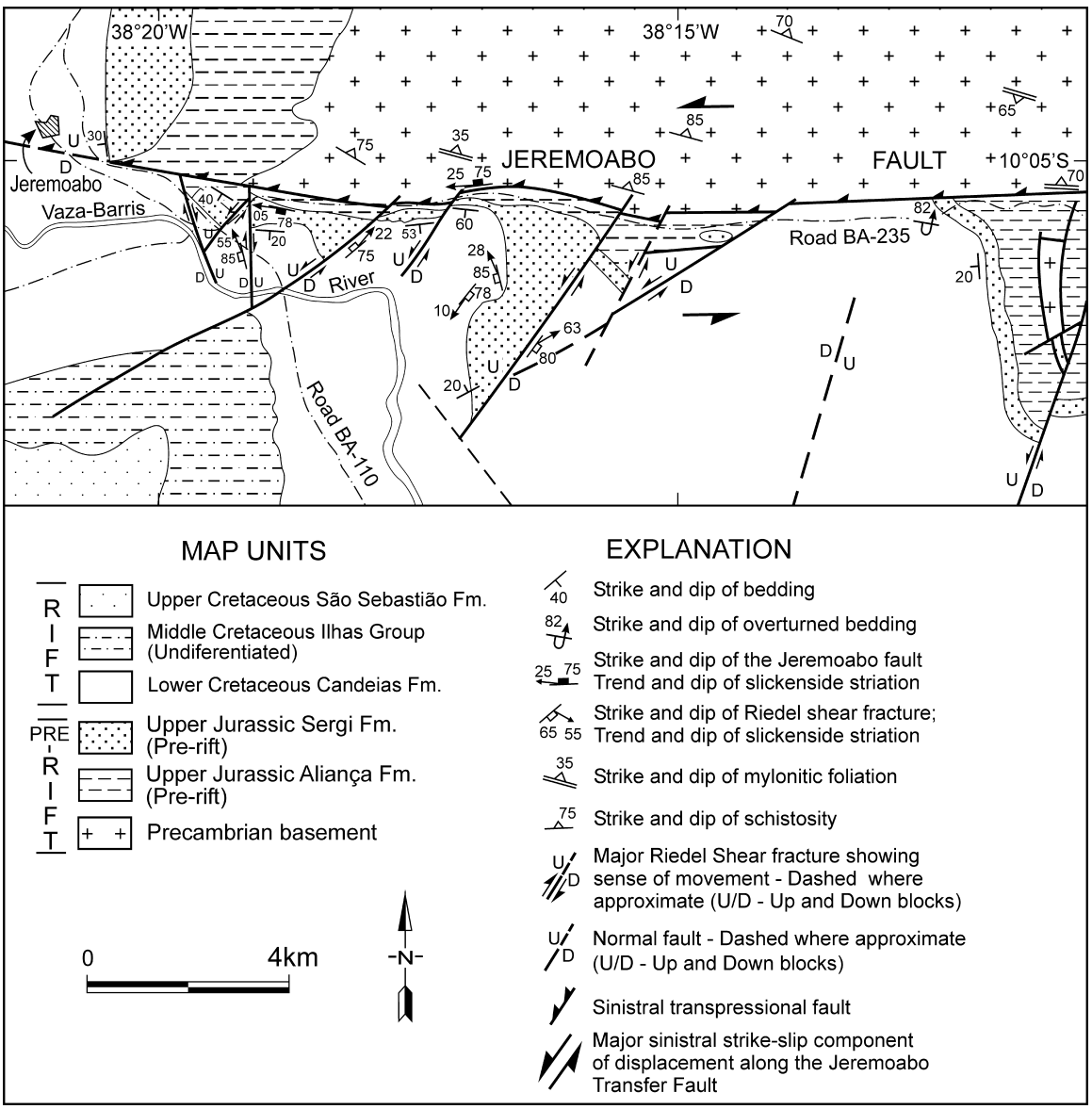

Fig. 4. Geologic map of the study area (modified from Magnavita and Cupertino, 1987; Menezes Filho et al., 1988). The major NE- and NNW-trending brittle faults represent a conjugate system of Riedel shear fractures.

ranging from Lower Neocomian to Lower Aptian are deformed by the Jeremoabo fault (Fig. 3). To the east of Jeremoabo town, sediments of the prerift Sergi and Aliança, and synrift Candeias formations, are cut by the fault (Fig. 3). To the west, these sediments and younger sandstones of the Ilhas group and the São Sebastião formation are also deformed by the fault (Fig. 3). Upper Aptian postrift sediments of the Marizal formation are not deformed by the rift faults (Fig. 3). Magnavita (1992) inferred a period of sinistral motion across the Jeremoabo fault during the Berriasian/Valanginian time.

3. The Jeremoabo fault and associated structures

The Jeremoabo fault is marked by a single and discrete steeply dipping brittle fault surface. Dipping about 70° to the north, the fault brings a slice of the Precambrian basement on top of Upper Jurassic sandstones. Its northward dip is reflected by the dip of foliation in the basement adjacent to the Belo Monte shear zone (Fig. 4). To the west of the Jeremoabo town the fault can be followed for over 15 km farther into the Tucano Rift, where it dies out (Fig. 2). Towards the east the fault surface merges with the Belo Monte shear zone. The geometry of the Jeremoabo fault surface was determined by combining field observations with data from aerial photographs and detailed and regional geologic maps by other authors (e.g. Menezes Filho et al., 1988; Davison and Santos, 1989).

The hanging wall block of the Jeremoabo fault consists mainly of Late Proterozoic rocks of the Sergipana Fold Belt, a meta-volcanoclastic sequence with serpentinized

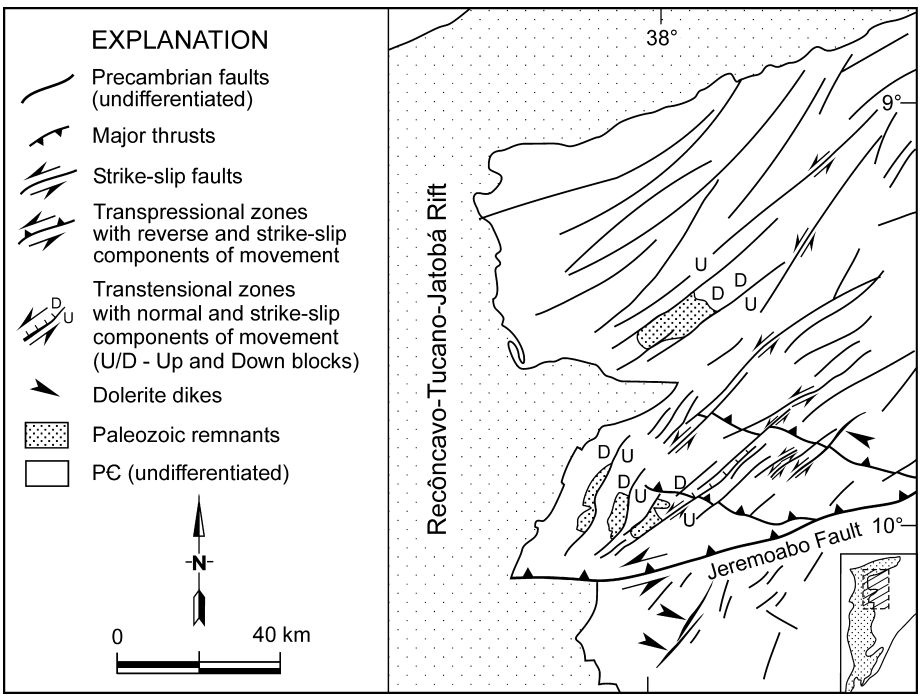

Fig. 5. Brittle shear zones in the basement east of the North Tucano Sub-basin, showing sinistral strike- and oblique-slip faults formed during rifting (Magnavita, 1992). Paleozoic remnants are preserved in the downthrown block of some of these faults.

ultramafic bodies, intruded by Brasiliano plutons (Magnavita, 1992). These rocks are cut by a number of NE-trending brittle faults, with an overall sinistral sense of displacement (Fig. 5). Sometimes, these faults show a normal component of movement, where sandstones of Paleozoic age are preserved (Magnavita, 1992) (Fig. 5). Magnavita (1992) proposed that these faults were generated during an Early Neocomian rifting event and affected a larger area, before deformation became more localized, and a main fracture prevailed along the present-day rifted basin. Magnavita (1992) also proposed that the movement on these NE-trending faults is related to sinistral simple shear, which is consistent with the motion observed across the Ibimirim border fault in the Jatobá Basin, and also accounts for the evolution of the Santa Brígida Graben (see Fig. 2). Dolerite dikes intruded along some of these sinistral faults that also occur both to the north and south of the Jeremoabo fault (Fig. 5).

A deformation zone about 5 km wide developed along the entire length of the footwall block (the Araticum block) of the Jeremoabo fault, involving sandstones and shales of both Upper Jurassic prerift and Cretaceous rift sequences (Fig. 4). The deformation zone consists of the Jeremoabo fault itself and associated structures, including drag-shaped folds and a system of conjugate oblique faults on outcrop to kilometer scale. These latter structures are particularly widespread in the strongly silicified Jurassic sandstones.

Bedding in the sandstone bodies of the Araticum Block is well defined by cross-stratified layers of coarse-grained sandstones, which are commonly separated by horizons of quartz-rich pebbly conglomerates. These sandstones are strongly lithified and commonly contain silicified wood fragments. Field description of outcrops and analysis of 1:50,000 scale aerial photographs indicate that bedding planes are deflected, becoming in some cases parallel to the fault surface.

According to the geometry of the deformed sandstone bodies, the study area can be divided into five blocks, labeled A–E (Fig. 6), bounded by a system of oblique faults. Stereographic plots and contoured stereograms representing poles to bedding for blocks A–E are shown in Fig. 6a–e. In blocks A and B bedding dips gently (ca. 20°), respectively, to the south and southwest. In block C bedding planes also dip south, but dip angles progressively increase with the proximity of the Jeremoabo fault. Block D encompasses the largest sandstone body, and displays the largest drag-shaped fold structure of the study area (Fig. 6). Block E also contains a drag-shaped fold where the beds become overturned and parallel to fault. Thus, a gradual increase in bedding rotation towards east and towards the basin margin can be recognized in the maps and stereoplots of Fig. 6. The axes of the footwall folds plunge gently towards W and WSW, as shown in the stereograms of Fig. 6. Synoptic stereographic plots of bedding poles (Fig. 6f) lie along a great-circle near the center of the stereogram, indicating that the drag-shaped fold structures are a result of rotation about an inclined axis plunging nearly 12° towards 268°. This suggests that movement along the Jeremoabo fault is oblique, with a strong vertical component of displacement.

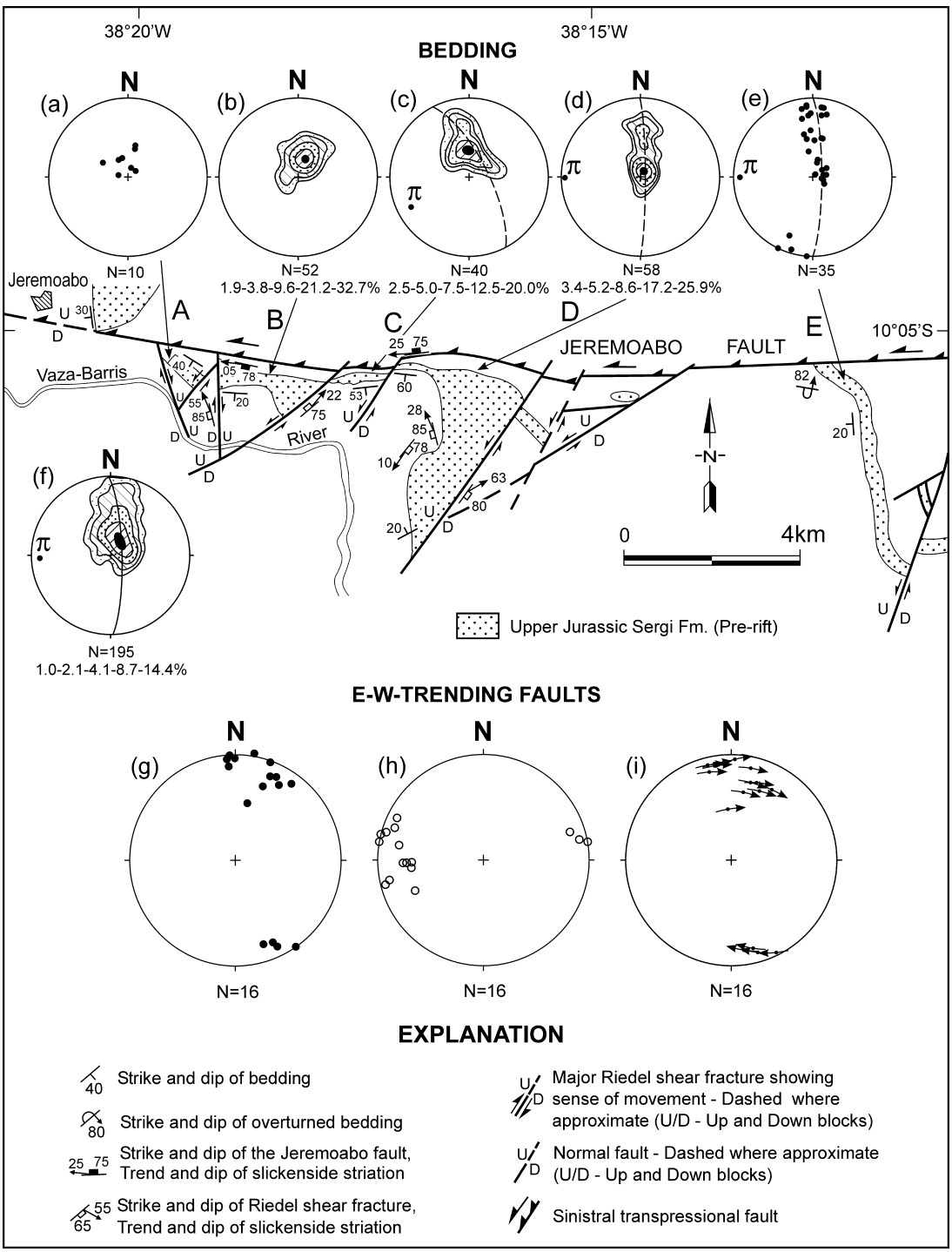

Fig. 6. Structural map of the study area, showing location of studied blocks along the Jeremoabo fault. (a)–(e) Equal-area lower-hemisphere stereograms of bedding poles for each block. Stereograms presenting smaller number of poles and/or greater dispersion are not contoured. Near the Jeremoabo fault the dips of bedding increase from W to E, and may be inverted in block E. Best-fit great circles and correspondent π-axes are shown for blocks C–E. π-axes plunge gently westwards, which give orientation of the major drag-shaped structures of these blocks and indicate sinistral movements. (f) Synoptic stereogram showing best-fit great circle to poles to bedding and the correspondent π-axis for the whole area. (g)–(i) Equal-area lower-hemisphere stereograms related to E–W-trending faults showing, respectively, poles to fault planes, plots to slickenside striations, and slip-linear plots. Note E–W-trending faults located near the Jeremoabo fault in blocks B and D.

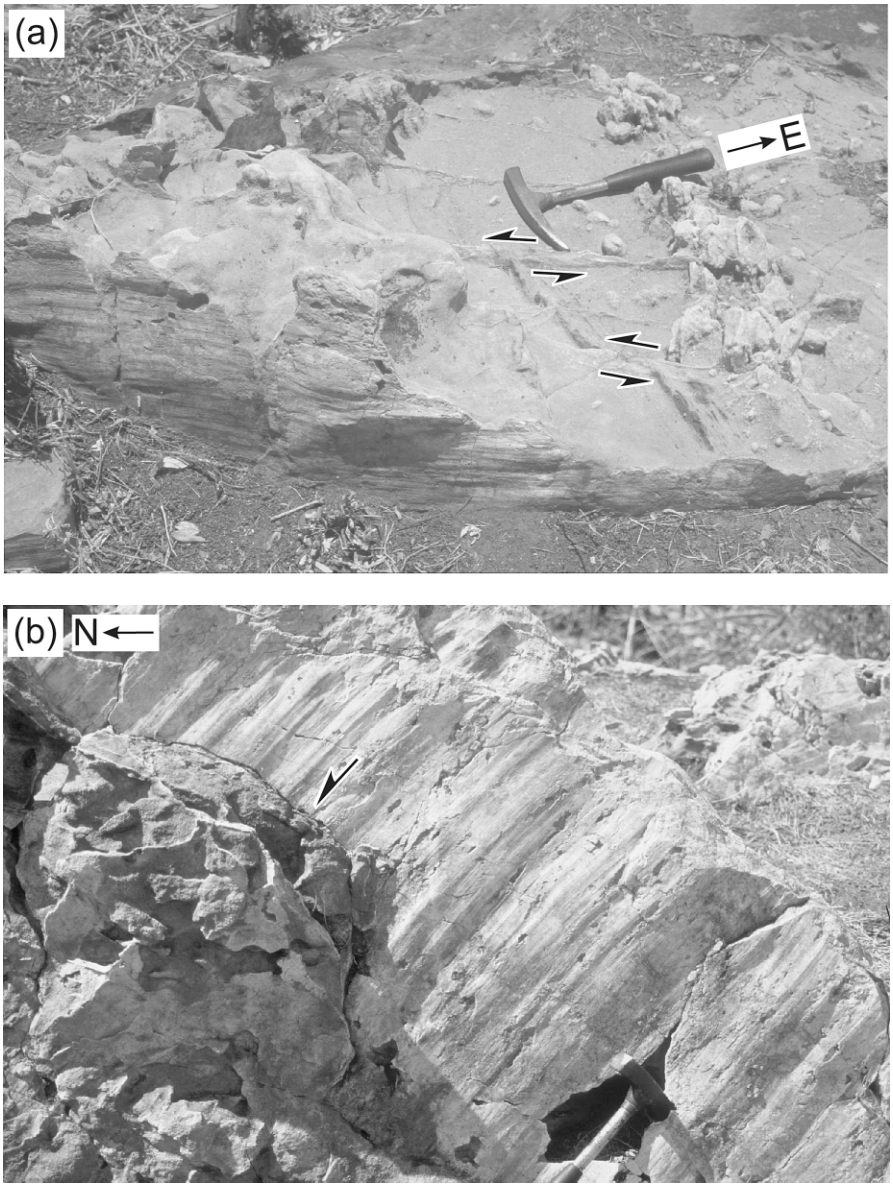

Fig. 7. (a) EW-trending fault surface located near and parallel to the Jeremoabo fault, showing subhorizontal slickenside striations (see site 1 in Fig. 8). Note sinistral faults dislocating ferruginous sandstone beds below the hammer. (b) N–S-trending fault plane bearing high-rake slickenside striations.

3.1. The Jeremoabo fault

E–W-trending fault surfaces parallel to the Jeremoabo fault are observed on deformation bands of millimetric to centimetric thicknesses (Fig. 7a). The discrete fault surfaces, commonly displaying slickenside striations, are observed internally or at the boundaries of the deformation bands, which are very well depicted in outcrops due to the cataclasis and silicification. These faults dip steeply (Figs. 6g and 7a) and have been found within the footwall block only in those portions of the sandstone blocks that are close to the main fault (Fig. 6). This indicates that the Jeremoabo fault itself follows a very narrow zone along the reactivated Belo Monte shear zone.

The slickenside striations on the E–W-trending faults show low rakes (Figs. 6h and 7a). In outcrops, the sense of movement along the Jeremoabo fault was deduced from kinematic indicators such as slickenside striations, offset bedding surfaces and offset deformation bands, which indicate a sinistral sense of shear (Fig. 7a). A slip-linear plot of the striations on these faults is shown in Fig. 6i, which is consistent with the sinistral movement along the Jeremoabo fault seen in Fig. 7a. We use slip-linear plots (Marshak and Mitra, 1988) because they are useful for representing the kinematics of fault arrays in the study area. A slip-linear plot is an equal-area plot on which the symbol for the pole to a fault plane is decorated by an arrow that indicates the direction and sense of slip. The arrows indicate the relative movement of the hanging wall block. The sinistral

movement observed on the Jeremoabo fault is in accordance with deflections of sandstone beds adjacent to the fault, which are consistent with a sinistral strike-slip component of movement (Fig. 6). For example, in the southern portions of the footwall blocks D and E shown in Fig. 6, sandstone beds strike about N–S and dip 20° W. To the north these beds are folded becoming parallel to the fault surface, thus exhibiting an overall left lateral rotation.

Although the sinistral offset of the rift border (about 20 km) between the footwall and the hanging wall (Fig. 6) might be original, it is more likely that the reverse-sinistral movement along the Jeremoabo fault generated at least part of this offset. The Araticum Block acted as a relatively

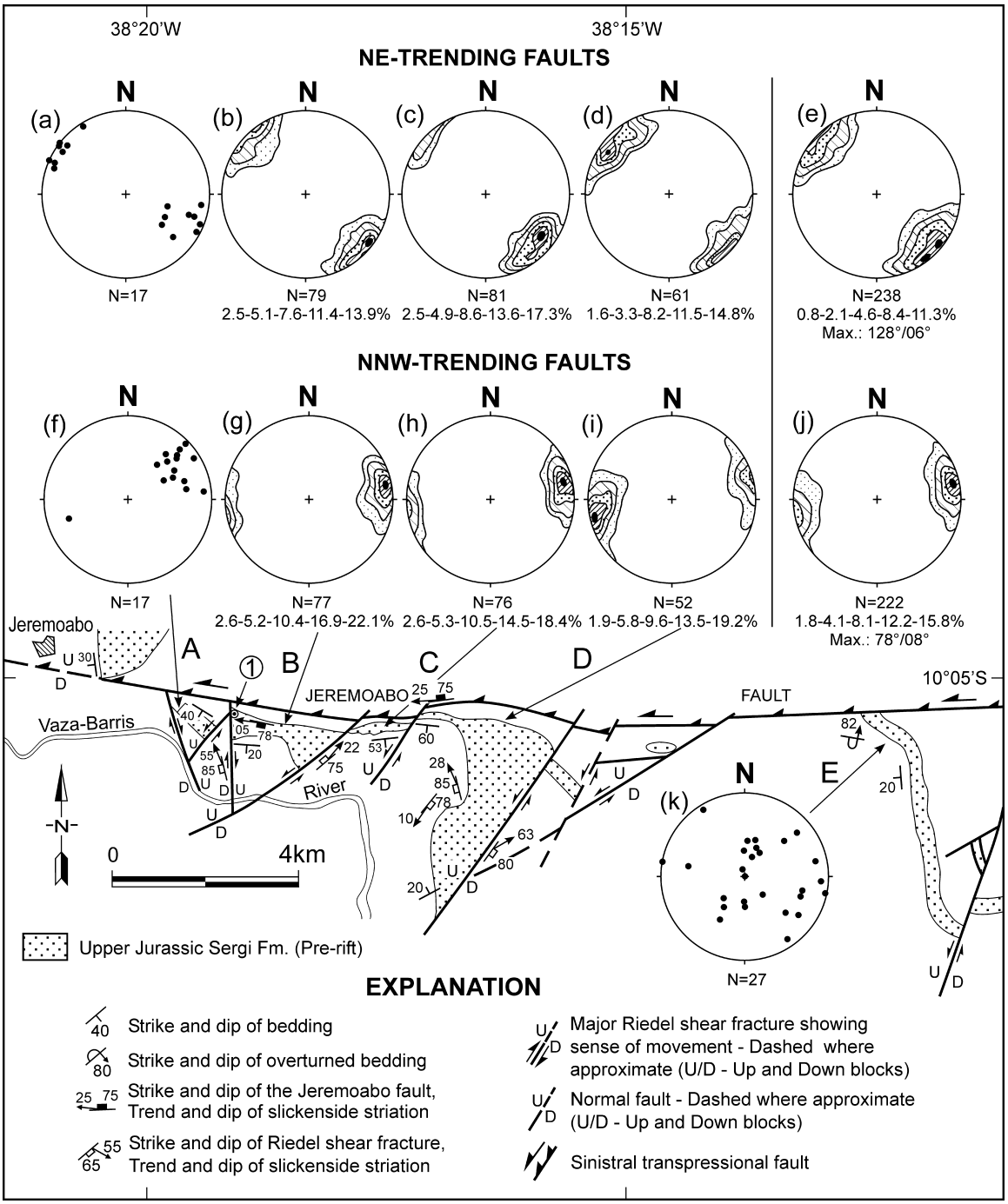

Fig. 8. Equal-area lower-hemisphere stereograms of plots to NE- ((a)–(d)) and NNW-trending faults ((f)–(i)) for blocks A–D. (e) and (j) are synoptic stereograms of, respectively, NE- and NNW-trending faults. Note that the fault planes of both fault systems dip steeply regardless the bedding rotation, especially in Blocks C and D (compare with Fig. 6). (k) Stereogram of poles to faults for block E.

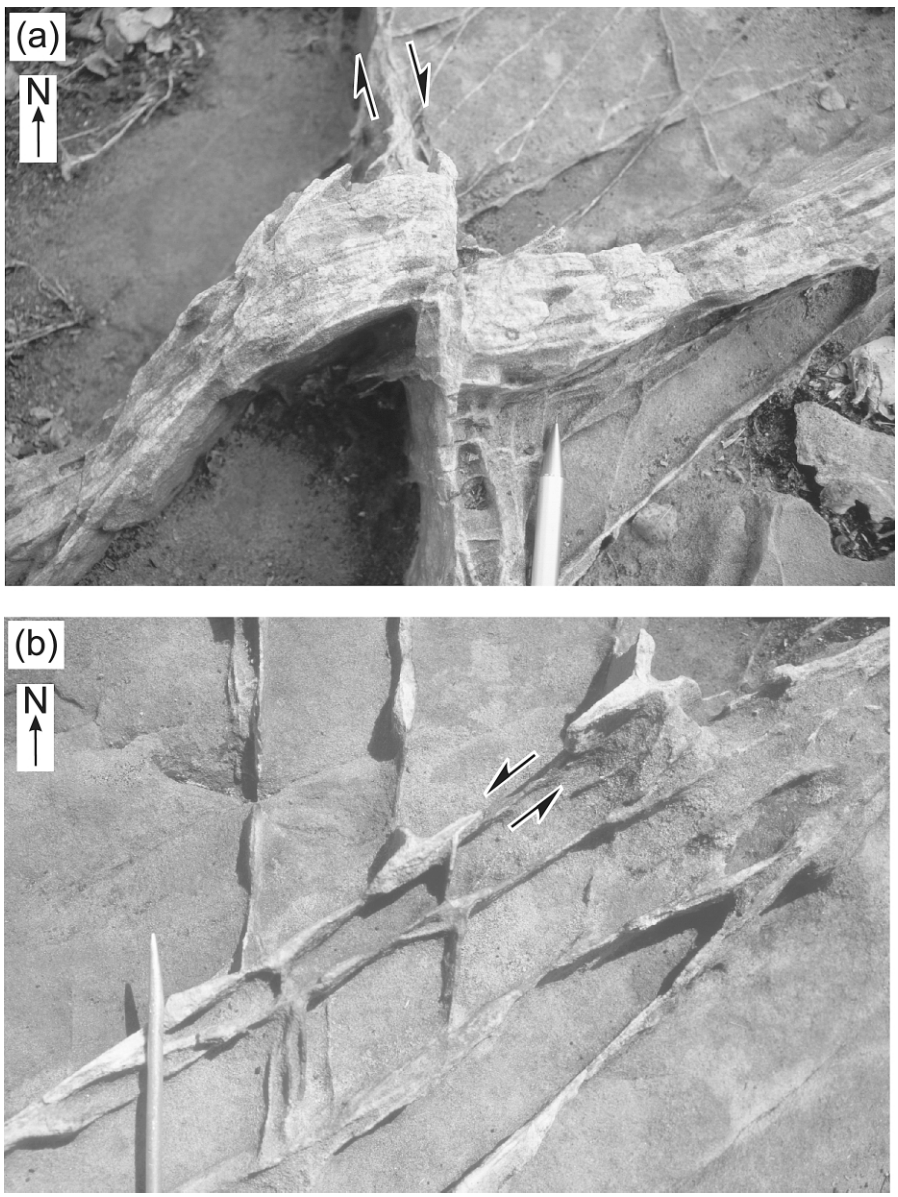

Fig. 9. Conjugate NNW- and NE-trending Riedel fractures dislocating each other by, respectively, (a) dextral movement and (b) sinistral movement.

stable block during the formation of the Jeremoabo fault. This is evidenced by the presence of only the most basal stratigraphic units of the rift (Fig. 3), which show mainly gentle dips. Although offset markers are not observed along the Jeremoabo fault, a vertical separation of no more than 1 km may have occurred across the fault, by considering the mapped offset of the basin border and bedding dips along the Jeremoabo fault.

3.2. Conjugate faults

A system of NE- and NNW-trending large-scale faults dominates the footwall Araticum Block (Fig. 8). The faults dip steeply (ca. 80°) in outcrops and show up on aerial photographs as pronounced topographic fault scarps, where the sandstone bodies are up to 30 m higher than the adjacent basement blocks. Conjugate sets of millimetric to centimetric deformation bands pervasively offset sandstone strata by several centimeters (Fig. 9a and b). Similarly to the E–W-trending faults, the discrete fault surfaces are observed internally or at the boundaries of the deformation bands. These faults reproduce on a smaller scale, the pattern of the faults that bound the previously described sandstone blocks. Locally, these deformation bands join together, thicken to several meters, and extend for hundreds of meters. NE- and NNW-trending fault sets are equally abundant in the study area, although one of them may predominate in individual outcrops.

The NE- and NNW-trending faults mutually offset each other, and are systematically and consistently observed in the whole study area. Acting as unequivocal mesoscopic-scale kinematic indicators the two fault systems are

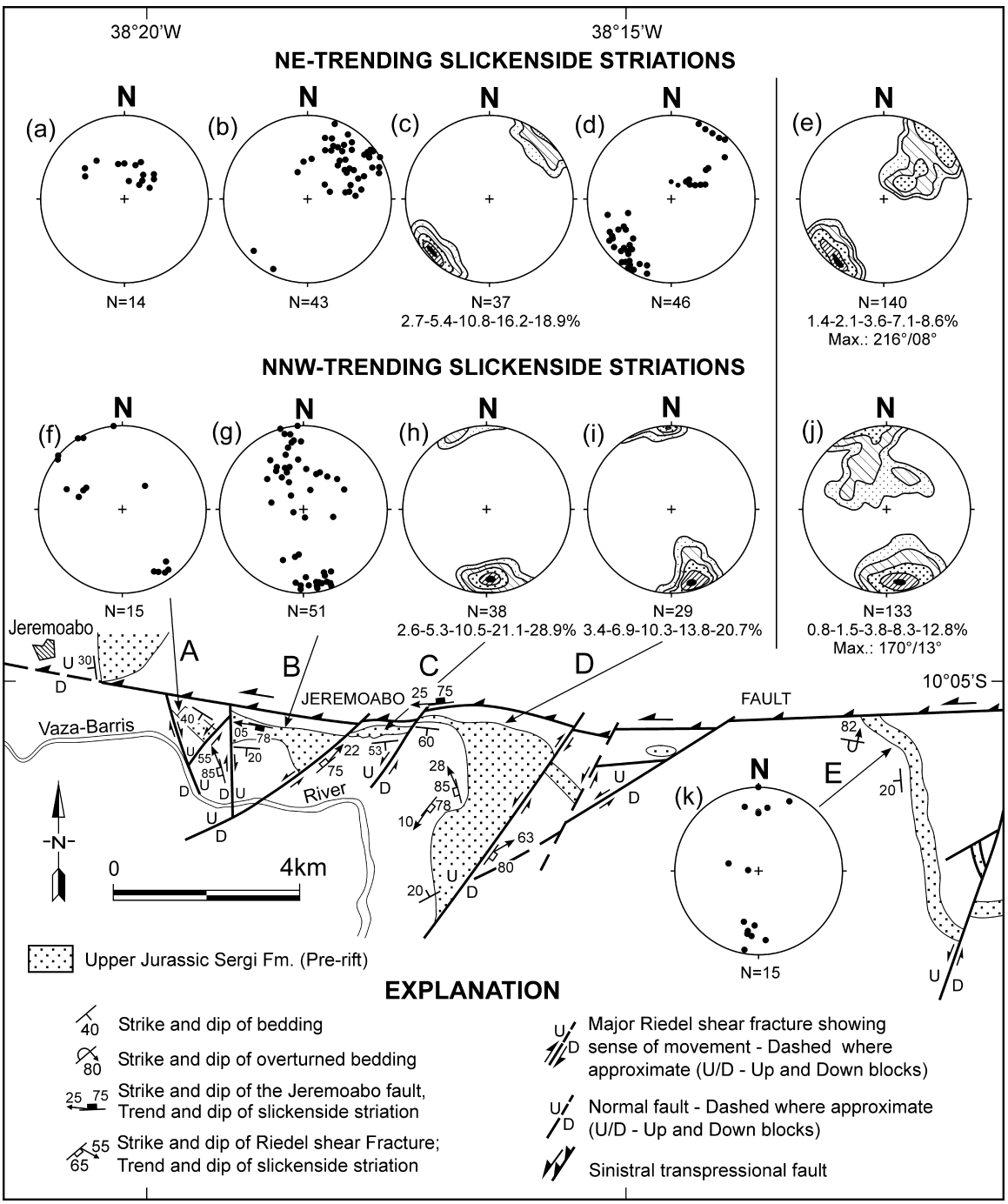

Fig. 10. Equal-area lower-hemisphere stereograms of plots to NE- ((a)–(d)) and NNW-trending slickenside striations ((f)–(i)) for blocks A–D. (e) and (j) are synoptic stereograms of, respectively, NE- and NNW-trending slickenside striations. Note that steeply dipping slickenside lineations generally dip northwards. (k) Stereogram of plots to slickenside striations for block E. They plunge gently and are located on the low angle faults of Fig. 8k.

subvertical and show, respectively, sinistral and dextral senses of displacement (Fig. 9a and b). The contoured stereograms and stereoplots in Fig. 8 represent these conjugate faults for blocks A–D. Unlike the other blocks, the faults in block E do not show a well-defined distribution (Fig. 8k). Although NE- and NNW-trending faults are observed in this block, a number of gently dipping faults also occur (Fig. 8k). These low angle faults probably formed during the southward movement of the hanging wall block of the Jeremoabo fault, as indicated by the steeply dipping bedding planes in this block, which may be overturned near the fault (Fig. 8). The lack of a well defined system of NE- and NNW-trending faults in outcrops in block E may be explained by the absence of confining kilometer-scale faults, which do exist in the other blocks.

The NE- and NNW-trending faults typically display

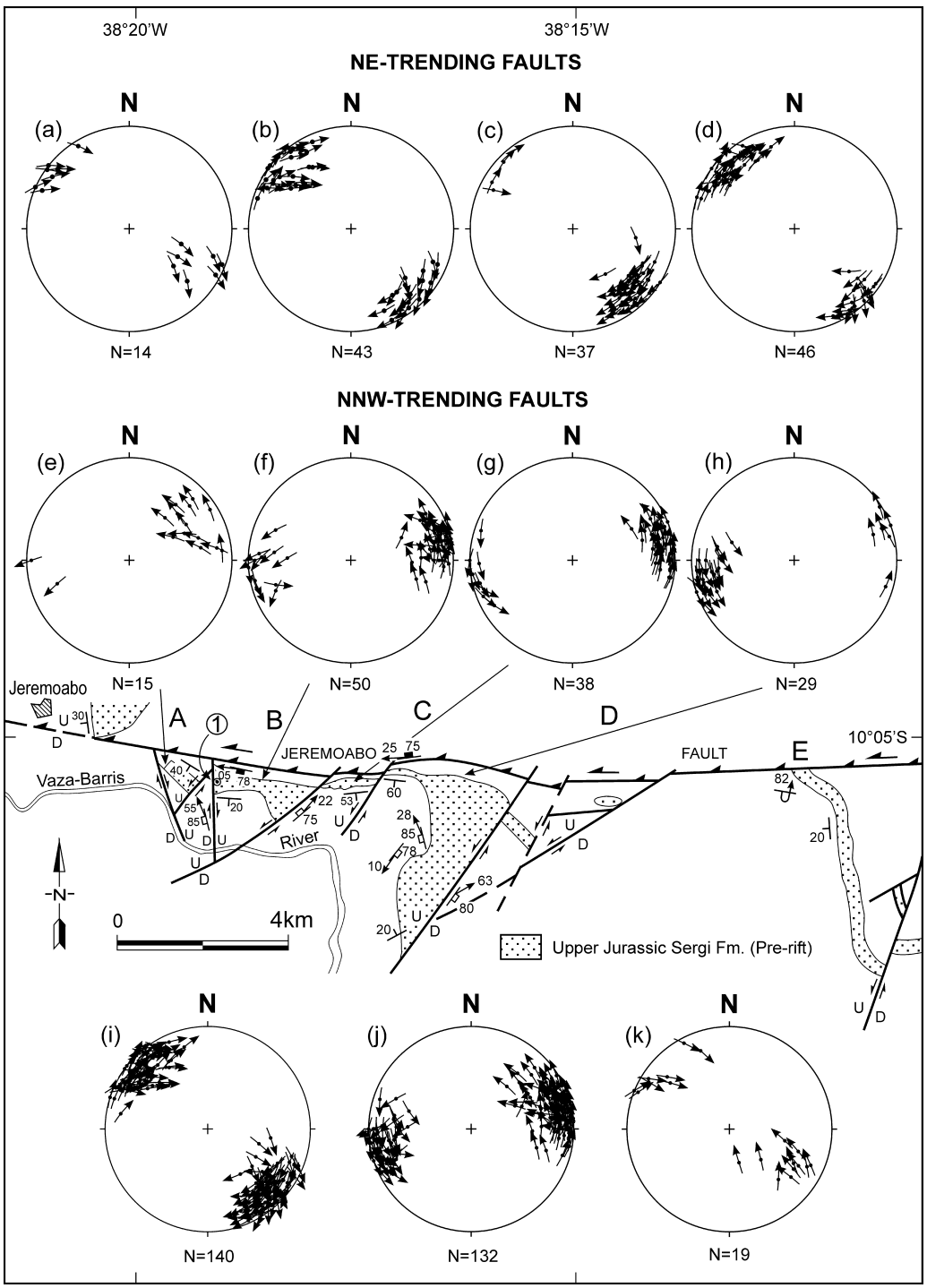

Fig. 11. Slip-linear plots to NE- ((a)–(d)) and NNW-trending faults ((e)–(h)) for blocks A–D. (i) and (j) Synoptic stereograms of, respectively, NE- and NNW-trending faults. Arrows at high angle to the equatorial circles of the stereograms represent steeply plunging slickenside striations. The ones pointing outside the stereograms are located on reverse-oblique faults, and the ones pointing inside the stereograms are located on faults presenting normal-oblique displacements (further explanation in the text). (k) Slip-linear plot for normal faults located in block B (locality 1). Note that the arrows from both fault sets dip towards the center of the stereogram, indicating normal displacements.

subhorizontal slickenside striations as shown in Fig. 7a. Fig. 10a–d and f–i show stereograms of plots of slickenside striations for blocks A–D. Fig. 10e and j show synoptic stereograms of these slickenside striations. High-rake striations, plunging about 60°, are also observed on the conjugate faults (Fig. 7b). They dip predominantly northwards, as shown in the stereograms of Fig. 10. These faults bearing high-rake striations commonly delimitate the individual sandstone blocks or are located near their boundaries, indicating that they probably acted as gliding

planes for the southward rotation of the sandstone packages during the development of drag folds, simultaneously with upward movement of blocks along these conjugate faults. A further analysis on the faults displaying these high-rake striations is given below. The slickenside striations of block E (Fig. 10k) are observed mainly on the low-angle faults shown in Fig. 8k and are also indicative of this movement, since in this block beds may be overturned and near parallel to the Jeremoabo fault (Fig. 10).

Slip-linear plots of the striations on both sinistral and dextral faults for each block are shown, respectively, in Fig. 11a–d and e–h. Stereograms of Fig. 11i and j are synoptic and reproduce the consistent sense of displacements observed in outcrops. Most arrows are parallel to the equatorial circle indicating the predominance of strike-slip movement. The arrows pointing outside and inside the stereograms represent high-rake striations, located on faults with, respectively, oblique reverse and oblique normal displacements.

Normal faults indicative of extension are scarce in the study area and are observed only in block B (site 1 in Fig. 11). They commonly form conjugate sets as shown by the arrows pointing in opposite directions and towards the center of the stereogram in Fig. 11k. We interpret these normal faults as having formed parallel to the compression direction deduced in the following section.

A preliminary interpretation about the conjugate faults bearing high-rake striations presented above suggested that they behaved as extensional normal faults, representing a transtensional switch in the orientation of the XY plane of bulk strains as predicted by theoretical models (e.g. Dewey et al., 1998). However, we systematically noted that the sense of movement shown by the kinematic indicators associated with these striations was contrary to that expected for extensional normal faults. Instead of being normal faults, they would thus act as high angle reverse faults and, even more surprisingly, bearing high-rake striations. Regardless of the dip direction of faults or the plunges of striations, the NE-trending faults are invariably sinistral and the NNW-trending faults, dextral. An example is given by the NE-trending fault population, located in the SE quadrant of the stereogram of Fig. 8e. We observed in the field that their horizontal component of motion is sinistral (Fig. 11i). The left-lateral sense combined with the northward plunge of the striations indicates an overall sinistral reverse displacement. The arrows pointing outside the stereogram of Fig. 11i show the reverse character of these faults. If they were normal faults, the arrows should point toward the center of the stereogram of Fig. 11i, as in Fig. 11k, which shows the normal faults observed in block B (site 1 in Fig. 11), the only ones observed in the study area. A similar analysis can be done for the NNW-trending fault population represented in the western portion of the stereogram of Fig. 8j, where the strike-slip component of movement of the steeply dipping faults bearing high-angle striations is invariably dextral reverse (Fig. 11j), as indicated by the arrows pointing outside the stereogram. Based on these evidences, we have considered that the conjugate faults bearing high angle striations represent steeply dipping reverse faults, instead of extensional normal faults. In stereograms of Fig. 11i and j, there are some arrows pointing inside the stereogram, indicating that their associated faults present normal displacements. These faults are also considered to have formed under bulk compression, integrating the fault sets analyzed above. The block diagram of Fig. 12 summarizes the kinematics of conjugate faults, showing the relative positions of both steeply and gently plunging slickenside striations for all blocks in the study area.

There is no evidence for rotation of the conjugate sets of faults expected to occur simultaneously with bedding rotation. This can be concluded from the analysis of blocks C and D, where the beds dip both gently and steeply, but faults are kept subvertical, showing no significant effect of bedding rotation (compare Figs. 6 and 8). Blocks C and D also present a predominance of low-rake striations (Fig. 10), which, just like the conjugate faults, were not significantly affected by bedding rotation. These facts suggest that most conjugate faults formed at a later stage, after bedding rotation and motion on the Jeremoabo fault, and on conjugate faults bordering the sandstone blocks, could no longer accommodate further shortening. This is shown in Fig. 11, where some large-scale conjugate faults offset the Jeremoabo fault. On the other hand, the faults displaying high-rake striations that delimitate blocks C and D, could also have acted as gliding planes, allowing the movement of blocks simultaneously with bedding rotation.

In blocks A and B beds dip gently (Fig. 6), many slickenside striations have low rakes, and others plunge steeply (Fig. 10), especially on the faults limiting the blocks. Since beds did not suffer marked rotation in these blocks, this may suggest that the steep plunges of these striations are mostly original, and that their orientation did not suffer significant changes during the deformation. This also supports the previous suggestion that the faults displaying these high-rake striations, which define the boundaries of the individual blocks, acted as gliding planes for the upward movement of the sandstone blocks. It can be seen in Fig. 12 that in blocks A and B, an upward rigid body translation predominated over southward bedding rotation, whereas in blocks C–E, southward rotation and upward translation were both important. Thus, the faults bearing high-rake striations located at the boundaries of the sandstone blocks would have acted as suitably oriented gliding planes for all blocks. Occasionally faults bearing high-rake striations may be observed within the sandstone blocks, and some low-rake striations may also be found at the boundaries of the blocks.

The events forming the structures observed in the study area can be summarized as follow:

1. In a first stage, conjugate sets of Riedel fractures with high-rake striations developed along the borders of the

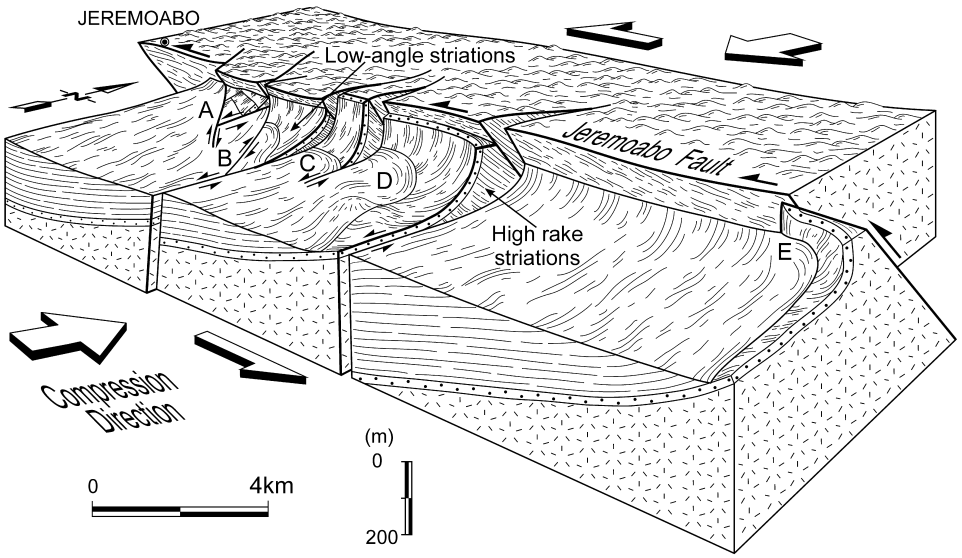

Fig. 12. Block-diagram representing the geometry and kinematics of the Jeremoabo fault. Note the southward rotation of sandstone blocks along the Jeremoabo fault. High-rake slickenside striations developed mainly on faults located at the boundaries of these blocks, whereas low-rake slickenside striations formed on faults located within the blocks. Note also that these high-rake striations dip northwards, as shown in the stereograms of Fig. 10. Large arrows indicate the compression direction and the bulk sinistral sense of displacement along the Jeremoabo fault.

sandstone blocks, simultaneously with southward rotation and upward translation of these blocks.

2. In a second stage, conjugate sets of Riedel fractures developed within the sandstone blocks, displaying low-rake striations. This occurred when bedding rotation and movement on the faults located at the boundaries of the sandstone blocks and bearing high-rake striations could no longer accommodate further shortening.

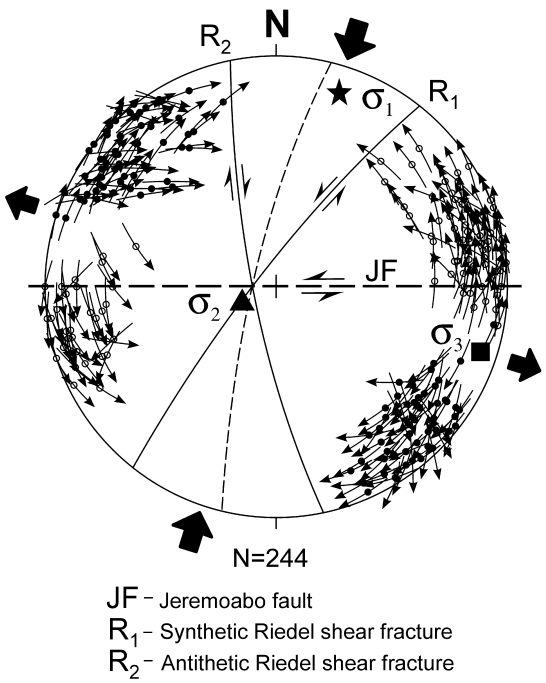

Fig. 13. Slip-linear plots for NE- and NNW-trending Riedel fractures. The principal stresses (σ_1, σ_2 and σ_3) were determined by using the Aleksandrowski's Method in the modified Goldstein and Marshak's (1988) version. The direction of σ_1 coincides with the bisector of the acute angle defined by the populations of the two fault systems (dashed line). Convergent and divergent large black arrows: directions of σ_1 and σ_3, respectively.

Because of their orientation, kinematics and relationship to the Jeremoabo fault, we have interpreted the previously described conjugate sets of faults as Riedel shear fractures genetically related to the sinistral Jeremoabo fault. In this context, the NE-trending set represents the synthetic R′ component, whereas the NNW-trending set corresponds to the antithetic R″ component.

4. The transpressional nature of the Jeremoabo fault

By applying Alexandrowski's (1985) method in Goldstein and Marshak's (1988) modified version, we have determined the direction of the principal paleostresses for the Jeremoabo fault. Because of their geometric and kinematic compatibility, we assumed for this analysis the previous interpretation that the Jeremoabo and the conjugate sets of faults are genetically related. The results obtained are shown in the diagram of Fig. 13. The maximum principal stress (σ_1) trends 016° and plunges 13° (Fig. 13). The minimum principal stress (σ_3) plunges 07° at 108°, whereas the intermediate principal stress (σ_2) plunges 76° at 244°. The bisectors of the modal strikes of the conjugate Riedel fractures give the orientations for σ_1 and σ_3 at about 012° and 104°, respectively, in accordance with the results of the paleostress method (Fig. 13). The angle between the

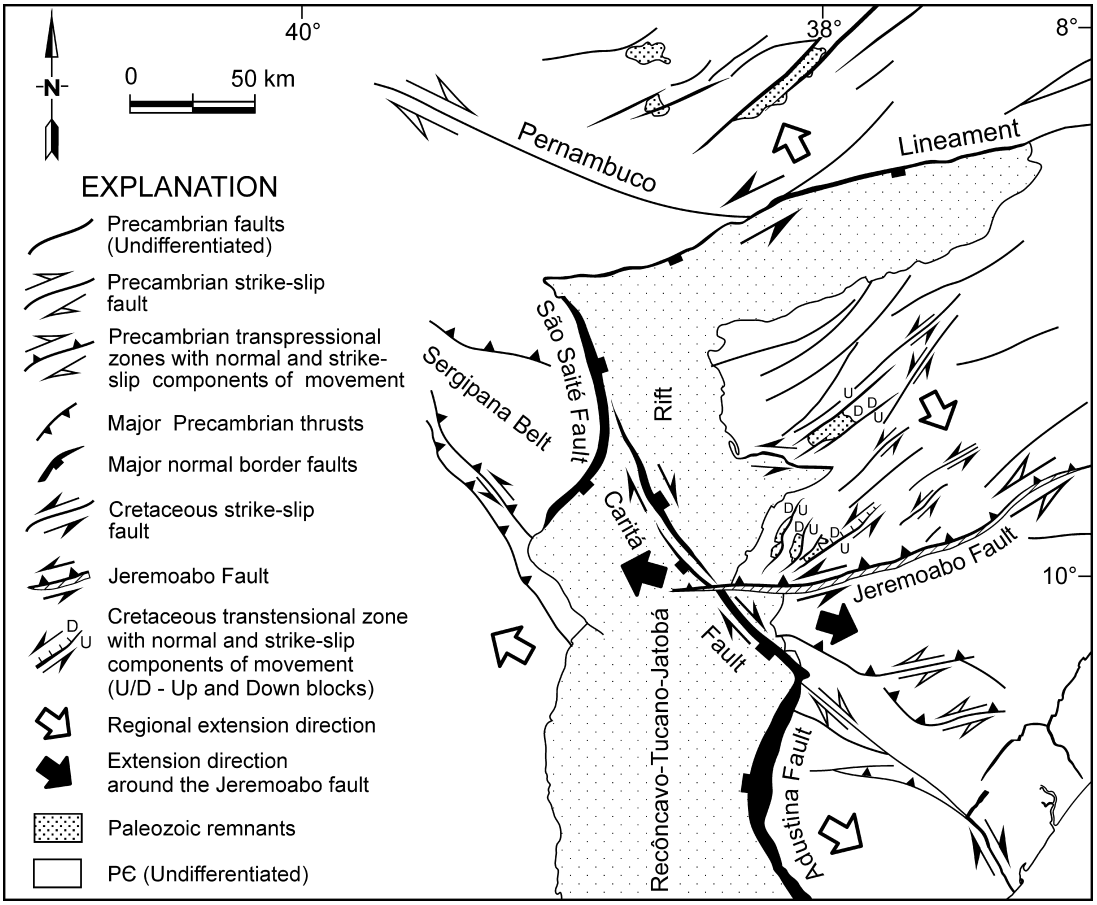

Fig. 14. Kinematic model for the study area (modified from Magnavita, 1992). Extension direction deduced for the Jeremoabo fault is WNW–ESE, while to the north and south of it, the bulk extension directions are, respectively, NNW–SSE and NW–SE.

deduced σ_1 and the Jeremoabo fault plane (ca. 75°) is consistent with a transpressional regime, as described by Sanderson and Marchini (1984). Besides showing lateral displacements, the hanging wall block was displaced vertically relative to the footwall block. This indicates that oblique simple shear (e.g. Dewey et al., 1998) occurred in the Jeremoabo fault.

As shown above, an overall NW–SE extension has been depicted for the Recôncavo–Tucano–Jatobá Rift, with σ_1 vertical. Since the paleostress analysis carried out above indicate that σ_2 was vertical along the Jeremoabo fault, we argue that the transpression along the Jeremoabo fault resulted from a local switch between the regional σ_1 and σ_2 maximum principal stresses, switching from a bulk extensional far-field stress state (σ_1 vertical), to a transpressional near-field stress state (σ_2 vertical) along the Jeremoabo fault.

5. Tectonic significance of the Jeremoabo fault

The stress perturbations near major pre-existent fault zones have been studied in several areas (e.g. Hudson and Cooling, 1988; Rawnsley et al., 1992; Sassi et al., 1993; Petit and Mattauer, 1995; Homberg et al., 1997). A basic assumption is that, depending on whether the discontinuity is open or rigid, the major principal stress may be diverted parallel to the discontinuity, may be unaffected, or may be diverted perpendicular to the discontinuity (e.g. Hudson and Cooling, 1988). Also, it is generally admitted that before new faults are formed, an ancient fault can be reactivated when its orientation with respect to the tectonic stresses is favorable and when the resistance on the pre-existing fault is less than the resistance to failure of the intact material (e.g. Sassi et al., 1993; Dewey et al., 1998). Thus, the transpressional reactivation of the Belo Monte shear zone, creating the Jeremoabo fault, probably occurred along a northward-dipping and suitably oriented discontinuity. This observation has led us to propose an alternative interpretation for the kinematics of the Jeremoabo fault, which is different from the models presented previously. We propose that the Jeremoabo fault, dipping northwards, allowed the northern basement block to be shifted westwards and thrusted southwards over the Araticum Block, thus acting as a reverse-sinistral fault (Fig. 12).

The local transpression responsible for the development of the Jeremoabo fault can be viewed as a consequence of the oblique nature of the Tucano Rift, generated by reactivation of N–S-trending São Francisco Craton and

NE-trending Borborema Province structures, in response to an overall NW–SE extension. Since the rift axis is N–S-oriented, an oblique rift developed (Fig. 14). In this context, the E–W-trending and N-dipping Monte Belo shear zone acted as a restraining domain, enabling transpression to occur. Fig. 14 shows that the overall NW–SE-oriented extension direction is diverted to a NNW–SSE-oriented direction of extension to the north of the Jeremoabo fault, probably caused by the presence of the NE-trending pre-existing weak zones. These different directions of extension also helped transpression to occur along the Jeremoabo fault. Other examples of Cretaceous reactivation of pre-existing structures by both transpression and transtension have been recognized in the Borborema Province (e.g. Bedregal, 1991; Destro et al., 1994; Françolin et al., 1994).

To the north of the Jeremoabo fault, pre-existing weak zones strongly controlled the geometry of the rifted blocks, as well as their kinematics, constraining their movements to the movement of adjacent blocks. Particularly, the pre-existing fabric in the Borborema Province seems to have played a special role. In this area many NE-trending Precambrian basement faults to the east of the North Tucano Sub-basin were reactivated as sinistral brittle faults during rifting (Magnavita, 1992) (Fig. 14). As shown above some of these faults show a normal component of movement, preserving sandstone blocks of Paleozoic age (Magnavita, 1992). In the footwall Araticum Block, on the other hand, the high angle between σ_1 and the Jeremoabo fault and the scarcity of normal faults in the study area indicate that it experienced a strong component of compression, acting as a relatively stable block during rifting.

As shown previously, the Jeremoabo fault presents a sense of slip consistent with the mapped offset of the rift border, and connects smaller border faults of the basin, with maximum throws of only a few hundreds of meters. The main border faults of the Central and North Tucano rifts, the Adustina and São Saité faults, respectively, are connected by the dextral Caritá fault (Fig. 14). Despite these considerations, the transfer function of the Jeremoabo fault in the Tucano Rift becomes clear by the examination of the map shown in Fig. 4, where the hanging wall block to the north of the fault is composed of rocks of the Precambrian basement, whereas the footwall to the south of the fault, the Araticum Block, is formed by rift and prerift sediments. Additionally, crosscutting relationships indicate that the Jeremoabo fault was active during rifting, therefore synchronous with the major normal faults and other transfer structures of the Tucano Rift.

According to the kinematic model by Magnavita (1992) for the Vaza-Barris Arch, during rifting, the Jeremoabo fault was sinistral and the Caritá fault dextral, and both acted simultaneously. Both our data for the Jeremoabo fault, and the data from the Caritá fault (D.V.F. Vasconcellos et al., in preparation) support this interpretation (Fig. 14). Also, following Magnavita (1992), we argue that there is an intimate relationship between the Jeremoabo fault and the tectonic evolution of the Vaza-Barris Arch. On the basis of this analysis we herein propose that the Jeremoabo fault can be considered as a kind of transfer fault in the sense of Gibbs (1984), and a type of hard-linked transfer fault, in the sense of Walsh and Watterson (1991).

6. Conclusions

1. The analysis of small-scale Riedel fractures, allied to the deformation of a monotonous sequence of sandstones, provides evidence for the reactivation of the Late Proterozoic Belo Monte shear zone of the Sergipana Fold Belt, resulting in the formation of the Jeremoabo fault.
2. The orientation of conjugate small-scale Riedel fractures indicates that the intermediate principal stress (σ_2) was subvertical, and the maximum and minimum principal stresses (σ_1) and (σ_3), respectively, were sub-horizontal. The regional orientation of the maximum principal stress (σ_1) was 016°. The extension direction inferred along the Jeremoabo fault was 108° (σ_3 direction).
3. Steeply dipping beds occur mainly near the Jeremoabo fault, where beds may be rotated, becoming parallel to the fault surface. Drag-shaped folds, together with offset bedding surfaces, offset deformation bands, as well as slickenside striations, indicate a sinistral sense of shear for the Jeremoabo fault.
4. This sinistral sense of shear, together with the pattern of conjugate Riedel shear fractures, indicate that the Belo Monte shear zone was reactivated by transpression with sinistral reverse displacement, and with high angle between the orientation of the shear zone and the maximum principal compressive stress (σ_1). Oblique movement along the Jeremoabo fault and the conjugate fault sets accommodated shortening, by along-strike southward rotation and upward rigid body translation of blocks, with very steep bedding dips near the Jeremoabo fault.
5. The age of the Jeremoabo fault is locally constrained from post-Late Jurassic to Early Aptian, since sediments of the whole rift sequence are deformed by the fault. Upper Aptian postrift sediments are not deformed by rift faults, due to cessation of rifting.
6. Transpression along the Jeremoabo fault derived from oblique rifting strongly controlled by N–S- to NE-trending pre-existent weak zones. Under this condition, the hanging wall block was forced to depart from the bulk NW–SE-oriented extension direction and, as a consequence, thrusted over the footwall Araticum Block, which evolved under strong confinement and small internal extension.
7. Acting together with the Caritá dextral normal fault and the Vaza-Barris Arch, the Jeremoabo fault accommodated the polarity inversion between the Central and North Tucano Sub-basins, acting as a hard-linkage transfer fault.

Acknowledgements

This paper is a result of a PhD project by Nivaldo Destro at the Ouro Preto Federal University, Brazil. This paper has benefited greatly by the many thorough and helpful comments and reviews by Luis C. Correa-Gomes, Robert Holdsworth, João Hippertt, and André A. Bender. We thank Petrobras for provision of financial support and permission to publish. Fernando F. Alkmim received support from CNPq (Brazilian Council for the Scientific and Technological Development), grant #300833/99-7.

References

Aleksandrowski, P., 1985. Graphical determination of principal stress directions for slickenside lineation populations: an attempt to modify Arthaud's method. Journal of Structural Geology 7, 73–82.

Almeida, F.F.M., Hasui, Y., Brito Neves, B.B., Fuck, R.A., 1981. Brazilian structural provinces. Earth Science Review, Special Issue 17, 1–29.

Aragão, M.A.N.F., Peraro, A.A., 1994. Elementos estruturais do rifte Tucano/Jatobá. 3° Simpósio sobre o Cretáceo do Brasil, Boletim, Rio Claro, pp. 161–164.

Bedregal, R.P., 1991. Estudo gravimétrico e estrutural da Bacia de Iguatu-CE. Unpublished M.Sc. Thesis, Universidade Federal de Ouro Preto, Minas Gerais, Brasil.

Bosworth, W., 1995. A high-strain rift model for the southern Gulf of Suez (Egypt). In: Lambiase, J.J. (Ed.), Hydrocarbon Habitats in Rift Basins. Geological Society Special Publication 80, pp. 75–102.

Davison, I., 1985. A field based study of the structural development of the Tucano and Jatobá basins. Petrobras, Salvador, internal report no. 108-5581, 14pp.

Davison, I., Santos, R.A., 1989. Tectonic evolution of the Sergipano Fold Belt, NE Brazil, during the Brasiliano Orogeny. Precambrian Research 45, 319–342.

Destro, N., 1995. Release fault: a variety of cross fault in linked extensional fault systems in the Sergipe–Alagoas Basin, NE Brazil. Journal of Structural Geology 17, 615–629.

Destro, N., Szatmari, P., Ladeira, E.A., 1994. Post-Devonian transpressional reactivation of a Proterozoic ductile shear zone in Ceará, NE Brazil. Journal of Structural Geology 16, 35–45.

Destro, N., Szatmari, P., Alkmim, F.F., Magnavita, L.P., 2003. Release faults, associated structures, and their control on petroleum trends in the Recôncavo Rift, northeast Brazil. American Association of Petroleum Geologists Bulletin, in press.

Dewey, J.F., Holdsworth, R.E., Strachan, R.A., 1998. Transpression and transtension zones. In: Holdsworth, R.E., Strachan, R.A., Dewey, J.F. (Eds.), Continental Transpressional and Transtensional Tectonics. Geological Society Special Publication 135, pp. 1–14.

Françolin, J.B.L., Cobbold, P.R., Szatmari, P., 1994. Faulting in the early Cretaceous Rio do Peixe basin (NE Brazil) and its significance for the opening of the Atlantic. Journal of Structural Geology 16, 647–661.

Gibbs, A.D., 1984. Structural evolution of extensional basin margins. Journal of the Geological Society 141, 609–620.

Gibbs, A.D., 1990. Linked fault families in basin formation. Journal of Structural Geology 12, 795–803.

Goldstein, A., Marshak, S., 1988. Analysis of fracture array geometry. In: Marshak, S., Mitra, G. (Eds.), Basic Methods of Structural Geology, Prentice Hall, New Jersey, pp. 246–267.

Homberg, C., Hu, J.C., Angelier, J., Bergerat, F., Lacombe, O., 1997. Characterization of stress perturbations near major fault zones: insights from 2-D distinct-element numerical modeling and field studies (Jura Mountains). Journal of Structural Geology 19, 703–718.

Hudson, J.A., Cooling, C.M., 1988. In situ rock stresses and their measurement in the UK—Part I. The current state of knowledge. International Journal of Rock Mechanics and Mining Sciences & Geomechanics Abstracts 25, 363–370.

Lister, G.S., Etheridge, M.A., Symonds, P.A., 1986. Detachment faulting and the evolution of the passive continental margins. Geology 14, 246–250.

McClay, K., Khalil, S., 1998. Extensional hard linkages, eastern Gulf of Suez, Egypt. Geology 26, 563–566.

Magnavita, L.P., 1992. Geometry and kinematics of the Recôncavo–Tucano–Jatobá Rift, NE Brazil: Ph.D. thesis, University of Oxford, England.

Magnavita, L.P., Cupertino, J.A., 1987. Concepção atual sobre as bacias do Tucano e Jatobá, nordeste do Brasil. Boletim de Geociências da Petrobras 1 (2), 119–134.

Marshak, S., Mitra, G., 1988. Basic Methods of Structural Geology, Prentice Hall, New Jersey.

Menezes Filho, N.R. de, Santos, R.A. dos, Souza, J.D. de, 1988. Programa levantamentos geológicos básicos do Brasil–Folha de Jeremoabo–Estado da Bahia. DNPM/CPRM project, Brasília, 113pp.

Mercio, S.R., 1996. Análise estrutural da porção emersa da Bacia de Camamu. M.Sc. Thesis, convênio Petrobras/Universidade Federal de Ouro Preto, Ouro Preto, Minas Gerais, Brasil.

Milani, E.J., Davison, I., 1988. Basement control, and transfer tectonics in the Recôncavo–Tucano–Jatobá rift, Northeast Brazil. Tectonophysics 154, 41–70.

Milani, E.J., Lana, M.C., Szatmari, P., 1988. Mesozoic rift basins around the northeast Brazilian microplate (Recôncavo–Tucano–Jatobá, Sergipe–Alagoas). In: Manzpeizer, W., (Ed.), Triassic–Jurassic Rifting: Continental Breakup and the Origin of the Atlantic Ocean and Passive Margins, Elsevier, Amsterdam, pp. 833–858.

Petit, J.-P., Mattauer, M., 1995. Paleostress superimposition deduced from mesoscale structures in limestone: the Matelles exposure, Languedoc, France. Journal of Structural Geology 17, 245–256.

Rawnsley, K.D., Rives, T., Petit, J.-P., 1992. Joint development in perturbed stress fields near faults. Journal of Structural Geology 14, 939–951.

Salah, M.G., Alsharhan, A.S., 1996. Structural influence on hydrocarbon entrapment in the Northwestern North Sea, Egypt. American Association of Petroleum Geologists Bulletin 80, 101–118.

Sanderson, D.J., Marchini, W.R.D., 1984. Transpression. Journal of Structural Geology 6, 449–458.

Sassi, W., Colletta, P., Balé, P., Paquereau, T., 1993. Modelling of structural complexity in sedimentary basins: the role of pre-existing faults in thrust tectonics. Tectonophysics 226, 97–112.

Szatmari, P., Milani, E.J., 1999. Microplate rotation in northeast Brazil during South Atlantic rifting: Analogies with Sinai microplate. Geology 27, 1115–1118.

Szatmari, P., Milani, E.J., Lana, M.C., Conceição, J.C., Lobo, A., 1985. How South Atlantic rifting affects Brazilian oil reserves distribution. Oil and Gas Journal 14, 107–113.

Szatmari, P., Françolin, J.B.L., Zanotto, O., Wolff, S., 1987. Evolução tectônica da margem equatorial brasileira. Revista Brasileira de Geociências 17, 180–188.

Walsh, J.J., Watterson, J., 1991. Geometric and kinematic coherence and scale effects in normal fault systems. In: Roberts, A.M., Yielding, G., Freeman, B. (Eds.), The Geometry of Normal Faults. Geological Society Special Publication 56, pp. 193–206.